6 Quantitative Visualization

6.1 Introduction

An imaging system collects radiation emitted by objects to make them visible. The radiation consists of a flow of particles or electromagnetic or acoustic waves. In classical computer vision scenes and illumination are taken and analyzed as they are given, but visual systems used in scientific and industrial applications require a different approach. There, the first task is to establish the quantitative relation between the object feature of interest and the emitted radiation. It is the aim of these efforts to map the object feature of interest with minimum possible distortion of the collected radiance by other parameters.

Figure 6.1 illustrates that both the incident ray and the ray emitted by the object towards the camera may be influenced by additional processes. The position of the object can be shifted by refraction of the emitted ray. Scattering and absorption of the incident and emitted rays lead to an attenuation of the radiant flux that is not caused by the observed object itself but by the environment, which thus falsifies the observation. In a proper setup it is important to ensure that these additional influences are minimized and that the received radiation is directly related to the object feature of interest. In cases where we do not have any influence on the illumination or setup, we can still choose radiation of the most appropriate type and wavelength range.

As illustrated in Sections 1.2 and 6.4, a wealth of phenomena is available for imaging objects and object features, including self-emission, induced emission (fluorescence), reflection, refraction, absorption, and scattering of radiation. These effects depend on the optical properties of the object material and on the surface structure of the object. Basically, we can distinguish between surface-related effects caused by discontinuity of optical properties at the surface of objects and volume-related effects.

It is obvious that the complexity of the procedures for quantitative visualization strongly depends on the image-processing task. If our goal is only to make a precise geometrical measurement of the objects, it is sufficient to set up an illumination in which the objects are uniformly illuminated and clearly distinguished from the background. In this case, it is not required that we establish quantitative relations between the object features of interest and the radiation emitted towards the camera.

B. Jähne, Digital Image Processing
ISBN 3-540-24035-7

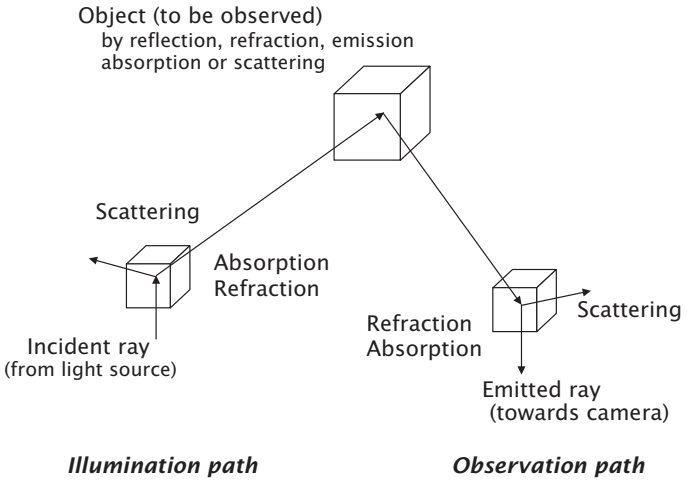

Figure 6.1: *Schematic illustration of the interaction between radiation and matter for the purpose of object visualization. The relation between the emitted radiation towards the camera and the object feature can be disturbed by scattering, absorption, and refraction of the incident and the emitted ray.*

If we want to measure certain object features, however, such as density, temperature, orientation of the surface, or the concentration of a chemical species, we need to know the exact relation between the selected feature and the emitted radiation. A simple example is the detection of an object by its color, i. e., the spectral dependency of the reflection coefficient.

In most applications, however, the relationship between the parameters of interest and the emitted radiation is much less evident. In satellite images, for example, it is easy to recognize urban areas, forests, rivers, lakes, and agricultural regions. But by which features do we recognize them? And, an even more important question, why do they appear the way they do in the images?

Likewise, in medical research one very general question of image-based diagnosis is to detect pathological aberrations. A reliable decision requires a good understanding of the relation between the biological parameters that define the pathological aberration and their appearance in the images.

In summary, essentially two questions must be answered for a successful setup of an imaging system:

1. How does the object radiance (emitted radiative energy flux per solid angle) depend on the object parameters of interest and illumination conditions?

2. How does the irradiance at the image plane (radiative energy flux density) captured by the optical system depend on the object radiance?

This chapter deals with the first of these questions, the second question is addressed in Section 7.5.

6.2 Radiometry, Photometry, Spectroscopy, and Color

6.2.1 Radiometry Terms

Radiometry is the topic in optics describing and measuring radiation and its interaction with matter. Because of the dual nature of radiation, the radiometric terms refer either to energy or to particles; in case of electromagnetic radiation, the particles are photons (Section 6.3.4). If it is required to distinguish between the two types, the indices e and p are used for radiometric terms.

Radiometry is not a complex subject. It has only become a confusing subject following different, inaccurate, and often even wrong usage of its terms. Moreover, radiometry is taught less frequently and less thoroughly than other subjects in optics. Thus, knowledge about radiometry is less widespread. However, it is a very important subject for imaging. Geometrical optics only tells us where the image of an object is located, whereas radiometry says how much radiant energy has been collected from an object.

Radiant Energy. Since radiation is a form of energy, it can do work. A body absorbing radiation is heated up. Radiation can set free electric charges in a suitable material designed to detect radiation. *Radiant energy* is denoted by Q and given in units of Ws (joule) or number of particles (photons).

Radiant Flux. The power of radiation, i. e., the energy per unit time, is known as *radiant flux* and denoted by Φ:

$$\Phi = \frac{\mathrm{d}Q}{\mathrm{d}t}. \tag{6.1}$$

This term is important to describe the total energy emitted by a light source per unit time. Its unit is joule/s (Js^{-1}), watt (W), or photons per s (s^{-1}).

Radiant Flux Density. The radiant flux per unit area, the flux density, is known by two names:

$$\text{irradiance} \quad E = \frac{\mathrm{d}\Phi}{\mathrm{d}A_0}, \quad \text{excitance} \quad M = \frac{\mathrm{d}\Phi}{\mathrm{d}A_0}. \tag{6.2}$$

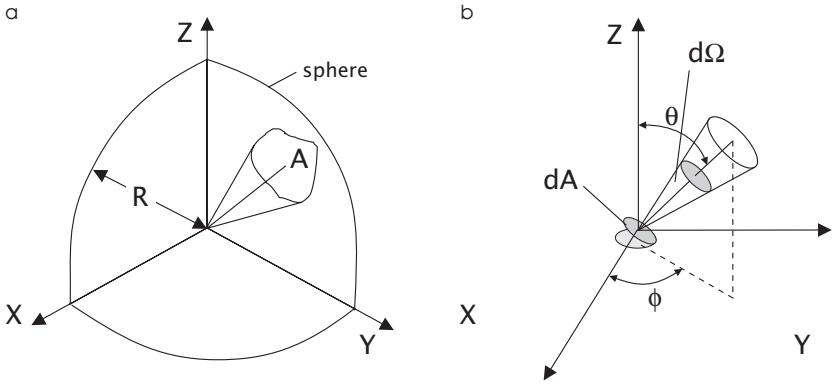

Figure 6.2: a *Definition of the solid angle.* ***b*** *Definition of radiance, the radiant power emitted per unit surface area* $\mathrm{d}A$ *projected in the direction of propagation per unit solid angle* Ω.

The *irradiance*, E, is the radiant flux incident upon a surface per unit area, for instance a sensor that converts the radiant energy into an electric signal. The unit of irradiance is $\mathrm{W\,m^{-2}}$, or photons per area and time ($\mathrm{m^{-2}s^{-1}}$). If the radiation is emitted from a surface, the radiant flux density is called *excitance* or *emittance* and denoted by M.

Solid Angle. The concept of the *solid angle* is paramount for an understanding of the angular distribution of radiation. Consider a compact source at the center of a sphere of radius R beaming radiation outwards in a cone of directions (Fig. 6.2a). The boundaries of the cone outline an area A on the sphere. The solid angle (Ω) measured in steradians (sr) is the area A divided by the square of the radius ($\Omega = A/R^2$). Although the steradian is a dimensionless quantity, it is advisable to use it explicitly when a radiometric term referring to a solid angle can be confused with the corresponding non-directional term. The solid angle of a whole sphere and hemisphere are 4π and 2π, respectively.

Radiant Intensity. The (total) radiant flux per unit solid angle emitted by a source is called the *radiant intensity* I:

$$I = \frac{\mathrm{d}\Phi}{\mathrm{d}\Omega}. \tag{6.3}$$

It is obvious that this term only makes sense for describing compact or point sources, i. e., when the distance from the source is much larger than its size. This region is also often called the far field of a radiator. Intensity is also useful for describing light beams.

Radiance. For an extended source, the radiation per unit area in the direction of excitance and per unit solid angle is an important quantity

(Fig. 6.2b):

$$L = \frac{\mathrm{d}^2\Phi}{\mathrm{d}A\,\mathrm{d}\Omega} = \frac{\mathrm{d}^2\Phi}{\mathrm{d}A_0 \cos\theta\,\mathrm{d}\Omega}. \tag{6.4}$$

The radiation can either be emitted from, pass through, or be incident on the surface. The radiance L depends on the angle of incidence to the surface, θ (Fig. 6.2b), and the azimuth angle ϕ. For a planar surface, θ and ϕ are contained in the interval $[0, \pi/2]$ and $[0, 2\pi]$, respectively. It is important to realize that the radiance is related to a unit area in the direction of excitance, $\mathrm{d}A = \mathrm{d}A_0 \cdot \cos\theta$. Thus, the effective area from which the radiation is emitted increases with the angle of incidence. The unit for energy-based and photon-based radiance are $\mathrm{W\,m^{-2}sr^{-1}}$ and $\mathrm{s^{-1}m^{-2}sr^{-1}}$, respectively.

Often, radiance — especially incident radiance — is called brightness. It is better not to use this term at all as it has contributed much to the confusion between radiance and irradiance. Although both quantities have the same dimension, they are quite different. Radiance L describes the angular distribution of radiation, while irradiance E integrates the radiance incident to a surface element over a solid angle range corresponding to all directions under which it can receive radiation:

$$E = \int_\Omega L(\theta,\phi)\cos\theta\,\mathrm{d}\Omega = \int_0^{\pi/2}\int_0^{2\pi} L(\theta,\phi)\cos\theta\sin\theta\,\mathrm{d}\theta\,\mathrm{d}\phi. \tag{6.5}$$

The factor $\cos\theta$ arises from the fact that the unit area for radiance is related to the direction of excitance (Fig. 6.2b), while the irradiance is related to a unit area parallel to the surface.

6.2.2 Spectroradiometry

Because any interaction between matter and radiation depends on the wavelength or frequency of the radiation, it is necessary to treat all radiometric quantities as a function of the *wavelength*. Therefore, we define all these quantities per unit interval of wavelength. Alternatively, it is also possible to use unit intervals of frequencies or wave numbers. The *wave number* denotes the number of wavelengths per unit length interval (see Eq. (2.14) and Section 2.3.6). To keep the various spectral quantities distinct, we specify the dependency explicitly, e. g., $L(\lambda)$, $L(\nu)$, and $L(k)$.

The radiometric terms discussed in the previous section measure the properties of radiation in terms of energy or number of photons. *Photometry* relates the same quantities to the human eyes' response to them. Photometry is of importance to scientific imaging in two respects: First, photometry gives a quantitative approach to radiometric terms as the human eye senses them. Second, photometry serves as a model for how

to describe the response of any type of radiation sensor used to convert irradiance into an electric signal. The key in understanding photometry is to look at the spectral response of the human eye. Otherwise, there is nothing new to photometry.

6.2.3 Spectral Sampling Methods

Spectroscopic imaging is in principle a very powerful tool for identifying objects and their properties because almost all optical material constants depend on the wavelength of the radiation. The trouble with spectroscopic imaging is that it adds another coordinate to imaging and the required amount of data is multiplied correspondingly. Therefore, it is important to sample the spectrum with the minimum number of samples sufficient to perform the required task. Here, we introduce several general spectral sampling strategies. In the next section, we also discuss human color vision from this point of view as one realization of spectral sampling.

Line sampling is a technique where each channel picks only a narrow spectral range (Fig. 6.3a). This technique is useful if processes are to be imaged that are related to emission or absorption at specific spectral lines. The technique is very selective. One channel "sees" only a specific wavelength and is insensitive — at least to the degree that such a narrow bandpass filtering can be realized technically — to all other wavelengths. Thus, this technique is suitable for imaging very specific effects or specific chemical species. It cannot be used to make an estimate of the total radiance from objects since it misses most wavelengths.

Band sampling is the appropriate technique if the total radiance in a certain wavelength range has to be imaged and still some wavelength resolution is required (Fig. 6.3b). Ideally, the individual bands have uniform responsivity and are adjacent to each other. Thus, band sampling gives the optimum resolution with a few channels but does not allow any distinction of the wavelengths within one band. The spectral resolution achievable with this sampling method is limited to the width of the spectral bands of the sensors.

In many cases, it is possible to make a model of the spectral radiance of a certain object. Then, a much better spectral sampling technique can be chosen that essentially samples not certain wavelengths but rather the parameters of the model. This technique is known as *model-based spectral sampling*.

We will illustrate this general approach with a simple example. It illustrates a method for measuring the mean wavelength of an arbitrary spectral distribution $\phi(\lambda)$ and the total radiative flux in a certain wave

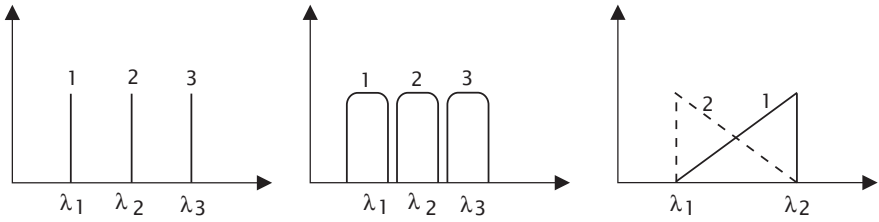

Figure 6.3: *Examples of spectral sampling:* ***a*** *line sampling,* ***b*** *band sampling,* ***c*** *sampling adapted to a certain model of the spectral range, in this example for a single spectral line of unknown wavelength.*

number range. These quantities are defined as

$$\phi = \frac{1}{\lambda_2 - \lambda_1} \int_{\lambda_1}^{\lambda_2} \phi(\lambda)\,\mathrm{d}\lambda \quad \text{and} \quad \overline{\lambda} = \int_{\lambda_1}^{\lambda_2} \lambda\phi(\lambda) d\lambda \Big/ \int_{\lambda_1}^{\lambda_2} \phi(\lambda)\,\mathrm{d}\lambda\,. \tag{6.6}$$

In the second equation, the spectral distribution is multiplied by the wavelength λ. Therefore, we need a sensor that has a sensitivity varying linearly with the wave number. We try two sensor channels with the following linear spectral *responsivity*, as shown in Fig. 6.3c:

$$\begin{aligned} R_1(\lambda) &= \frac{\lambda - \lambda_1}{\lambda_2 - \lambda_1} R_0 = \left(\frac{1}{2} + \tilde{\lambda}\right) R_0 \\ R_2(\lambda) &= R_0 - R_1(\lambda) = \left(\frac{1}{2} - \tilde{\lambda}\right) R_0, \end{aligned} \tag{6.7}$$

where R is the responsivity of the sensor and $\tilde{\lambda}$ the normalized wavelength

$$\tilde{\lambda} = \left(\lambda - \frac{\lambda_1 + \lambda_2}{2}\right) / (\lambda_2 - \lambda_1). \tag{6.8}$$

$\tilde{\lambda}$ is zero in the middle and $\pm 1/2$ at the edges of the interval.

The sum of the responsivity of the two channels is independent of the wavelength, while the difference is directly proportional to the wavelength and varies from $-R_0$ for $\lambda = \lambda_1$ to R_0 for $\lambda = \lambda_2$:

$$\begin{aligned} R_1'(\tilde{\lambda}) &= R_1(\lambda) + R_2(\lambda) = R_0 \\ R_2'(\tilde{\lambda}) &= R_1(\lambda) - R_2(\lambda) = 2\tilde{\lambda} R_0. \end{aligned} \tag{6.9}$$

Thus the sum of the signals from the two sensors R_1 and R_2, gives the total radiative flux, while the mean wavelength is given by $2\tilde{\lambda} = (R_1 - R_2)/(R_1 + R_2)$. Except for these two quantities, the sensors cannot reveal any further details about the spectral distribution.

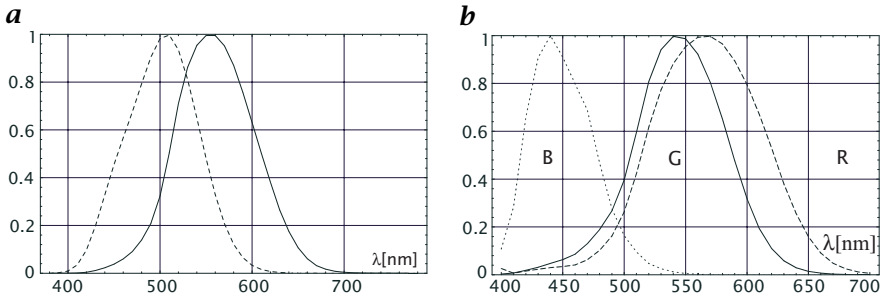

Figure 6.4: ***a*** *Relative spectral response of the "standard" human eye as set by the CIE in 1980 under medium to high irradiance levels (photopic vision, $V(\lambda)$, solid line), and low radiance levels (scotopic vision, $V'(\lambda)$, dashed line); data from [117].* ***b*** *Relative cone sensitivities of the human eye after DeMarco et al. [32].*

6.2.4 Human Color Vision

The *human visual system* responds only to electromagnetic radiation having wavelengths between about 360 and 800 nm. It is very insensitive at wavelengths between 360 and about 410 nm and between 720 and 830 nm. Even for individuals without vision defects, there is some variation in the spectral response. Thus, the visible range in the electromagnetic spectrum (light, Fig. 6.6) is somewhat uncertain.

The retina of the eye onto which the image is projected contains two general classes of receptors, rods and cones. Photopigments in the outer segments of the receptors absorb radiation. The absorbed energy is then converted into neural electrochemical signals which are transmitted via subsequent neurons and the optic nerve to the brain. Three different types of photopigments in the cones make them sensitive to different spectral ranges and, thus, enable color vision (Fig. 6.4b). Vision with cones is only active at high and medium illumination levels and is also called *photopic vision*. At low illumination levels, vision is taken over by the rods. This type of vision is called *scotopic vision*.

At first glance it might seem impossible to measure the spectral response of the eye in a quantitative way since we can only rely on the subjective impression how the human eye senses "radiance". However, the spectral response of the human eye can be measured by making use of the fact that it can sense brightness differences very sensitively. Based on extensive studies with many individuals, in 1924 the International Lighting Commission (CIE) set a standard for the spectral response of the human observer under photopic conditions that was slightly revised several times later on. Figure 6.4 show the 1980 values. The relative spectral response curve for scotopic vision, $V'(\lambda)$ is similar in shape but the peak is shifted from about 555 nm to 510 nm (Fig. 6.4a).

Physiological measurements can only give a relative spectral luminous efficiency function. Therefore, it is required to set a new unit for luminous quantities. This new unit is the candela; it is one of the seven fundamental units of the metric system (Système Internationale, or SI). The candela is defined to be the luminous intensity of a monochromatic source with a frequency of 5.4×10^{14} Hz and a radiant intensity of 1/683 W/sr. The odd factor 1/683 has historical reasons because the candela was previously defined independently from radiant quantities.

With this definition of the luminous intensity and the capability of the eye to detect small changes in brightness, the luminous intensity of any light source can be measured by comparing it to a standard light source. This approach, however, would refer the luminous quantities to an individual observer. Therefore, it is much better to use the standard spectral luminous efficacy function. Then, any luminous quantity can be computed from its corresponding radiometric quantity by:

$$\begin{aligned} Q_v &= 683 \frac{\mathrm{lm}}{\mathrm{W}} \int_{380\,\mathrm{nm}}^{780\,\mathrm{nm}} Q(\lambda) V(\lambda)\, \mathrm{d}\lambda \qquad \text{photopic,} \\ Q_{v'} &= 1754 \frac{\mathrm{lm}}{\mathrm{W}} \int_{380\,\mathrm{nm}}^{780\,\mathrm{nm}} Q(\lambda) V'(\lambda)\, \mathrm{d}\lambda \quad \text{scotopic,} \end{aligned} \tag{6.10}$$

where $V(\lambda)$ is the spectral luminous efficacy for day vision (photopic). A list with all photometric quantities and their radiant equivalent can be found in Appendix A (≻ R15). The units of luminous flux, the photometric quantity equivalent to radiant flux (units W) is lumen (lm).

In terms of the spectral sampling techniques summarized above, human color vision can be regarded as a blend of band sampling and model-based sampling. The sensitivities cover different bands with maximal sensitivities at 445 nm, 535 nm, and 575 nm, respectively, but which overlap each other significantly (Fig. 6.4b). In contrast to our model examples, the three sensor channels are unequally spaced and cannot simply be linearly related. Indeed, the color sensitivity of the human eye is uneven, and all the nonlinearities involved make the science of color vision rather difficult. Here, we give only some basic facts in as much as they are useful to handle color images.

With three-color sensors, it is obvious that color signals cover a 3-D space. Each point in this space represents one color. It is clear that many spectral distributions, known as *metameric color stimuli* or just metameres, map onto one point in the color space. Generally, we can write the signal s_i received by a sensor with a spectral responsivity $R_i(\lambda)$ as

$$s_i = \int R_i(\lambda) \phi(\lambda)\, \mathrm{d}\lambda. \tag{6.11}$$

With three primary color sensors, a triple of values is received, often called a *tristimulus*.

One of the most important questions in *colorimetry* is how to set up a system representing colors as linear combination of some basic or *primary colors*. A set of three spectral distributions $\phi_j(\lambda)$ represents a set of primary colors and results in an array of responses that can be described by the matrix P with

$$p_{ij} = \int R_i(\lambda)\phi_j(\lambda)\,\mathrm{d}\lambda. \tag{6.12}$$

Each vector $\boldsymbol{p}_j = (p_{1j}, p_{2j}, p_{3j})$ represents a tristimulus of the primary colors in the 3-D color space. It is obvious that only colors can be represented that are a linear combination of the base vectors $\boldsymbol{p}_j$

$$\boldsymbol{s} = R\boldsymbol{p}_1 + G\boldsymbol{p}_2 + B\boldsymbol{p}_3 \qquad \text{with} \qquad 0 \le R, G, B \le 1, \tag{6.13}$$

where the coefficients are denoted by R, G, and B, indicating the three primary colors red, green, and blue. Only if the three base vectors $\boldsymbol{p}_j$ are an orthogonal base can all colors be presented as a linear combination of them. One possible and easily realizable primary color system is formed by the monochromatic colors red, green, and blue with wavelengths 700 nm, 546.1 nm, and 435.8 nm, as adopted by the CIE in 1931. In the following, we use the primary color system according to the European EBU norm with red, green, and blue phosphor, as this is the standard way color images are displayed.

Given the significant overlap in the spectral response of the three types of cones (Fig. 6.4b), especially in the green image, it is obvious that no primary colors exist that can span the color systems. The colors that can be represented lie within the parallelepiped formed by the three base vectors of the primary colors. The more the primary colors are correlated with each other, i. e., the smaller the angle between two of them, the smaller is the color space that can be represented by them. Mathematically, colors that cannot be represented by a set of primary colors have at least *one* negative coefficient in Eq. (6.13).

One component in the 3-D color space is intensity. If a color vector is multiplied by a scalar, only its intensity is changed but not the color. Thus, all colors could be normalized by the intensity. This operation reduces the 3-D color space to a 2-D color plane or chromaticity diagram:

$$r = \frac{R}{R+G+B}, \quad g = \frac{G}{R+G+B}, \quad b = \frac{B}{R+G+B}, \tag{6.14}$$

$$\text{with} \qquad r + g + b = 1. \tag{6.15}$$

It is sufficient to use only the two components r and g. The third component is then given by $b = 1 - r - g$, according to Eq. (6.15). Thus, all colors that can be represented by the three primary colors R, G, and

B are confined within a triangle in the rg space as shown in Fig. 6.5a. As already mentioned, some colors cannot be represented by the primary colors. The boundary of all possible colors is given by the visible monochromatic colors from deep red to blue. The line of monochromatic colors forms a U-shaped curve in the rg-space. Because all colors that lie on a straight line between two colors can be generated as an additive mixture of these colors, the space of all possible colors covers the area filled by the U-shaped spectral curve and the straight mixing line between its two end points for blue and red color (purple line).

In order to avoid negative color coordinate values, often a new coordinate system is chosen with virtual primary colors, i. e., primary colors that cannot be realized by any physical colors. This color system is known as the *XYZ color system* and constructed in such a way that it just includes the curve of monochromatic colors with only positive coefficients (Fig. 6.5c) and given by the following linear coordinate transform:

$$\begin{bmatrix} X \\ Y \\ Z \end{bmatrix} = \begin{bmatrix} 0.490 & 0.310 & 0.200 \\ 0.177 & 0.812 & 0.011 \\ 0.000 & 0.010 & 0.990 \end{bmatrix} \begin{bmatrix} R \\ G \\ B \end{bmatrix}. \tag{6.16}$$

The back-transform from the XYZ color system to the RGB color system is given by the inverse of the matrix in Eq. (6.16).

The color systems discussed so far do not directly relate to the human sense of color. From the rg or xy values, we cannot directly infer colors such as green or blue. A natural type of description of colors includes besides the *luminance* (*intensity*) the type of color, such as green or blue (*hue*) and the purity of the color (*saturation*). From a pure color, we can obtain any degree of saturation by mixing it with white.

Hue and saturation can be extracted from chromaticity diagrams by simple coordinate transformations. The point of reference is the white point in the middle of the chromaticity diagram (Fig. 6.5b). If we draw a line from this point to a pure (monochromatic) color, it constitutes a mixing line for a pure color with white and is thus a line of constant hue. From the white point to the pure color, the saturation increases linearly. The *white point* is given in the rg chromaticity diagram by $w = [1/3, 1/3]^T$.

A color system that has its center at the white point is called a *color difference system*. From a color difference system, we can infer a hue-saturation color system (hue, saturation, and density; HIS) by simply using polar coordinate systems. Then, the saturation is proportional to the radius and the hue to the angle (Fig. 6.5b).

So far, color science is easy. All the real difficulties arise from the need to adapt the color system in an optimum way to display and print devices and for transmission by television signals or to correct for the uneven color resolution of the human visual system that is apparent in

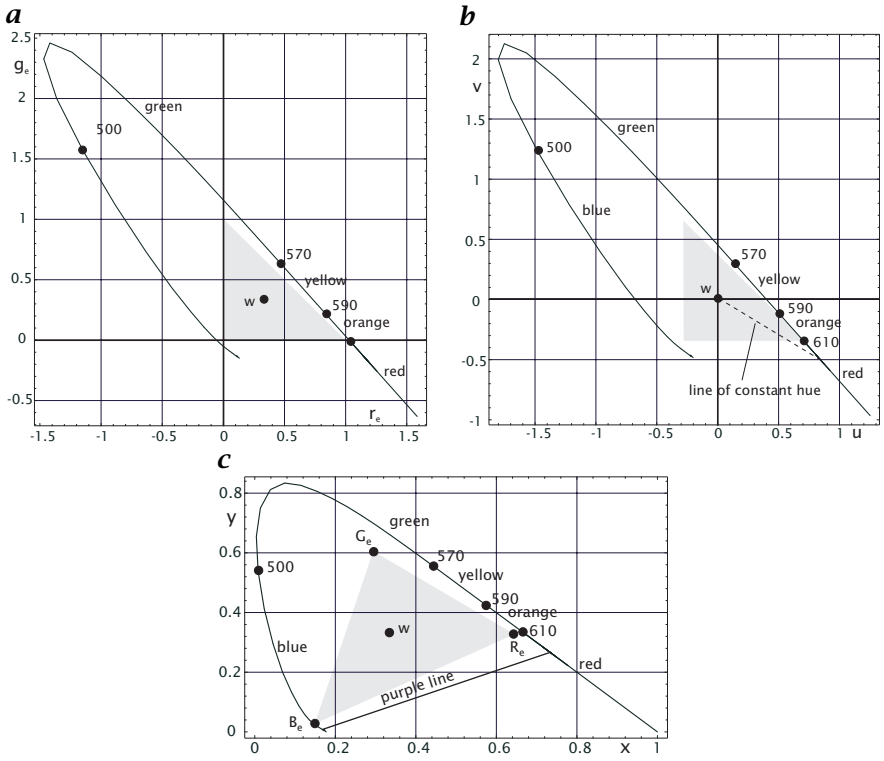

Figure 6.5: *Chromaticity diagram shown in the* **a** rg*-color space,* **b** uv*-color space,* **c** xy*-color space; the shaded triangles indicate the colors that can be generated by additive color mixing using the primary colors R, G, and B.*

the chromaticity diagrams of simple color spaces (Fig. 6.5). These needs have led to a confusing variety of different color systems (≻ R16).

6.3 *Waves and Particles*

Three principal types of radiation can be distinguished: electromagnetic radiation, particulate radiation with atomic or subatomic particles, and acoustic waves. Although these three forms of radiation appear at first glance quite different, they have many properties in common with respect to imaging. First, objects can be imaged by any type of radiation emitted by them and collected by a suitable imaging system.

Second, all three forms of radiation show a wave-like character including particulate radiation. The *wavelength* λ is the distance of one cycle of the oscillation in the propagation direction. The wavelength also governs the ultimate resolution of an imaging system. As a rule of thumb only structures larger than the wavelength of the radiation can be resolved.

Given the different types of radiation, it is obvious that quite different properties of objects can be imaged. For a proper setup of an image system, it is therefore necessary to know some basic properties of the different forms of radiation. This is the purpose of this section.

6.3.1 *Electromagnetic Waves*

Electromagnetic radiation consists of alternating *electric* and *magnetic fields*. In an *electromagnetic wave*, these fields are directed perpendicular to each other and to the direction of propagation. They are classified by the *frequency* ν and *wavelength* λ. In free space, all electromagnetic waves travel with the *speed of light*, $c \approx 3 \times 10^8$ ms^{-1}. The propagation speed establishes the relation between wavelength λ and frequency ν of an electromagnetic wave as

$$\boxed{\lambda\nu = c.} \tag{6.17}$$

The frequency is measured in cycles per second (Hz or s^{-1}) and the wavelength in meters (m).

As illustrated in Fig. 6.6, electromagnetic waves span an enormous frequency and wavelength range of 24 decades. Only a tiny fraction from about 400–700 nm, about one octave, falls in the visible region, the part to which the human eye is sensitive. The classification usually used for electromagnetic waves (Fig. 6.6) is somewhat artificial and has mainly historical reasons given by the way these waves are generated or detected.

In matter, the electric and magnetic fields of the electromagnetic wave interact with the electric charges, electric currents, electric fields, and magnetic fields in the medium. Nonetheless, the basic nature of electromagnetic waves remains the same, only the propagation of the wave is slowed down and the wave is attenuated.

The simplest case is given when the medium reacts in a linear way to the disturbance of the electric and magnetic fields caused by the electromagnetic wave and when the medium is isotropic. Then the influence of the medium is expressed in the complex *index of refraction*, $\eta = n + \mathrm{i}\chi$. The real part, n, or ordinary index of refraction, is the ration of the speed of light, c, to the propagation velocity u in the medium, $n = c/u$. The imaginary component of η, χ, is related to the attenuation of the wave amplitude.

Generally, the index of refraction depends on the frequency or wavelength of the electromagnetic wave. Therefore, the propagation speed of a wave is no longer independent of the wavelength. This effect is called *dispersion* and the wave is called a dispersive wave.

The index of refraction and the attenuation coefficient are the two primary parameters characterizing the optical properties of a medium. In the context of imaging they can be used to identify a chemical species or any other physical parameter influencing it.

Electromagnetic waves are generally a linear phenomenon. This means that we can decompose any complex wave pattern into basic ones such as plane harmonic waves. Or, conversely, we can superimpose any two or more electromagnetic waves and be sure that they are still electromagnetic waves.

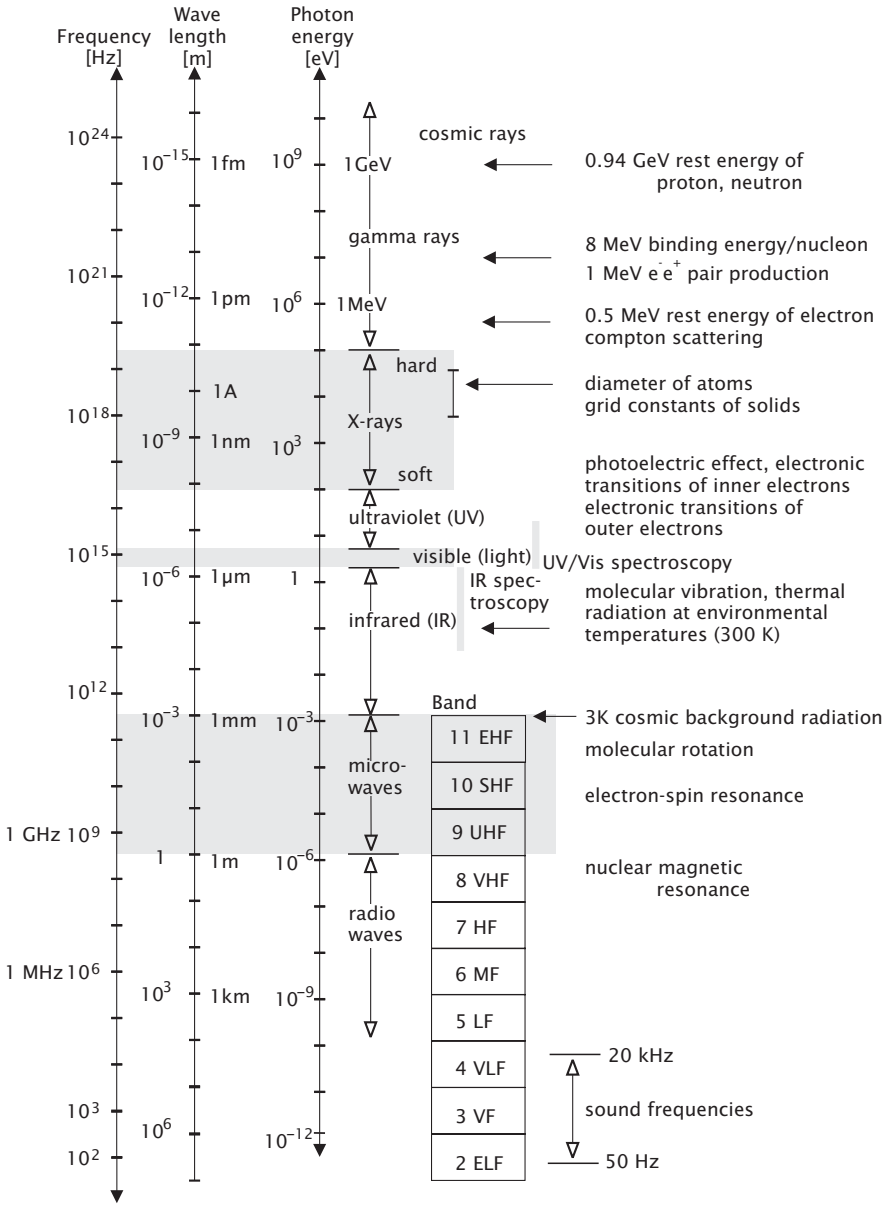

Figure 6.6: *Classification of the electromagnetic spectrum with wavelength, frequency, and photon energy scales.*

This superposition principle only breaks down for waves with very high field strengths. Then, the material no longer acts in a linear way on the electromagnetic wave but gives rise to *nonlinear optical phenomena*. These phenomena have become obvious only quite recently with the availability of very intense light sources such as lasers. A prominent nonlinear phenomenon is the *frequency doubling* of light. This effect is now widely used in lasers to produce output beams of double the frequency (half the wavelength). From the perspective of quantitative visualization, these nonlinear effects open an exciting new world for visualizing specific phenomena and material properties.

6.3.2 *Polarization*

The superposition principle can be used to explain the polarization of electromagnetic waves. Polarization is defined by the orientation of the electric field vector $\boldsymbol{E}$. If this vector is confined to a plane, as in the previous examples of a plane harmonic wave, the radiation is called *plane polarized* or *linearly polarized*. In general, electromagnetic waves are not polarized. To discuss the general case, we consider two waves traveling in the z direction, one with the electric field component in the x direction and the other with the electric field component in the y direction. The amplitudes E_1 and E_2 are constant and ϕ is the phase difference between the two waves. If $\phi = 0$, the electromagnetic field vector is confined to a plane. The angle ϕ of this plane with respect to the x axis is given by

$$\phi = \arctan \frac{E_2}{E_1}. \tag{6.18}$$

Another special case arises if the phase difference $\phi = \pm 90^\circ$ and $E_1 = E_2$; then the wave is called *circularly polarized*. In this case, the electric field vector rotates around the propagation direction with one turn per period of the wave. The general case where both the phase difference is not $\pm 90^\circ$ and the amplitudes of both components are not equal is called *elliptically polarized*. In this case, the E vector rotates in an ellipse, i. e., with changing amplitude around the propagation direction. It is important to note that any type of polarization can also be composed of a right and a left circular polarized beam. A left circular and a right circular beam of the same amplitude, for instance, combine to form a linear polarized beam. The direction of the polarization plane depends on the phase shift between the two circularly polarized beams.

6.3.3 *Coherence*

An important property of some electromagnetic waves is their *coherence*. Two beams of radiation are said to be *coherent* if a systematic relationship between the phases of the electromagnetic field vectors exists. If this relationship is random, the radiation is *incoherent*. It is obvious that incoherent radiation superposes in a different way than coherent radiation. In case of coherent radiation, destructive inference is possible in the sense that waves quench each other in certain places were the phase shift is 180°.

Normal light sources are incoherent. They do not send out one continuous planar wave but rather wave packages of short duration and with no particular phase relationship. In contrast, a laser is a coherent light source.

6.3.4 *Photons*

Electromagnetic radiation has particle-like properties in addition to those characterized by wave motion. Electromagnetic energy is quantized in that for a given frequency its energy can only occur in multiples of the quantity $h\nu$ in which h is *Planck's constant*, the *action quantum*:

$$\boxed{E = h\nu.} \tag{6.19}$$

The quantum of electromagnetic energy is called the *photon*.
In any interaction of radiation with matter, be it absorption of radiation or emission of radiation, energy can only be exchanged in multiples of these quanta. The energy of the photon is often given in the energy unit electron volts (eV). This is the kinetic energy an electron would acquire in being accelerated through a potential difference of one volt. A photon of yellow light, for example, has an energy of approximately 2 eV. Figure 6.6 includes a photon energy scale in eV. The higher the frequency of electromagnetic radiation, the more its particulate nature becomes apparent, because its energy quanta get larger. The energy of a photon can be larger than the energy associated with the rest mass of an elementary particle. In this case it is possible for electromagnetic energy to be spontaneously converted into mass in the form of a pair of particles. Although a photon has no rest mass, a momentum is associated with it, since it moves with the speed of light and has a finite energy. The momentum, p, is given by

$$p = h/\lambda. \tag{6.20}$$

The quantization of the energy of electromagnetic waves is important for imaging since sensitive radiation detectors can measure the absorption of a *single* photon. Such detectors are called photon counters. Thus, the lowest energy amount that can be detected is $h\nu$. The random nature of arrival of photons at the detector gives rise to an uncertainty ("noise") in the measurement of radiation energy. The number of photons counted per unit time is a *random variable* with a *Poisson distribution* as discussed in Section 3.4.1. If N is the average number of counted photons in a given time interval, the Poisson distribution has a standard deviation $\sigma_N = \sqrt{N}$. The measurement of a radiative flux with a relative standard deviation of 1 % thus requires the counting of 10 000 photons.

6.3.5 *Particle Radiation*

Unlike electromagnetic waves, most *particulate radiation* moves at a speed less than the speed of light because the particles have a non-zero rest mass. With respect to imaging, the most important type of particulate radiation is due to *electrons*, also known as *beta radiation* when emitted by radioactive elements. Other types of important particulate radiation are due to the positively charged nucleus of the hydrogen atom or the *proton*, the nucleus of the helium atom or *alpha radiation* which has a double positive charge, and the *neutron*.
Particulate radiation also shows a wave-like character. The wavelength λ and the frequency ν are directly related to the energy and momentum of the particle:

$$\begin{aligned} \nu &= E/h \quad \text{Bohr frequency condition,} \\ \lambda &= h/p \quad \text{de Broglie wavelength relation.} \end{aligned} \tag{6.21}$$

These are the same relations as for the photon, Eqs. (6.19) and (6.20). Their significance for imaging purposes lies in the fact that particles typically have much shorter wavelength radiation. Electrons, for instance, with an energy of 20 keV have a wavelength of about 10^{-11} m or 10 pm, less than the diameter of atoms (Fig. 6.6) and about 50 000 times less than the wavelength of light. As the resolving power of any imaging system — with the exception of nearfield systems — is limited to scales in the order of a wavelength of the radiation (Section 7.6.3), imaging systems based on electrons such as the *electron microscope*, have a much higher potential resolving power than any light microscope.

6.3.6 *Acoustic Waves*

In contrast to electromagnetic waves, *acoustic* or *elastic waves* need a carrier. Acoustic waves propagate elastic deformations. So-called *longitudinal acoustic waves* are generated by isotropic pressure, causing a uniform compression and thus a deformation in the direction of propagation. The local density ρ, the local pressure p and the local velocity $\boldsymbol{v}$ are governed by the same wave equation

$$\frac{\partial^2 \rho}{\partial t^2} = u^2 \Delta \rho, \quad \frac{\partial^2 p}{\partial t^2} = u^2 \Delta p, \qquad \text{with} \quad u = \frac{1}{\sqrt{\rho_0 \beta_{ad}}}, \tag{6.22}$$

where u is the velocity of sound, ρ_0 is the static density and β_{ad} the *adiabatic compressibility*. The adiabatic compressibility is given as the relative volume change caused by a uniform pressure (force/unit area) under the condition that no heat exchange takes place:

$$\beta_{ad} = -\frac{1}{V}\frac{\mathrm{d}V}{\mathrm{d}P}. \tag{6.23}$$

Thus the *speed of sound* is related in a universal way to the elastic properties of the medium. The lower the density and the compressibility, the higher is the speed of sound. Acoustic waves travel much slower than electromagnetic waves. Their speed in air, water, and iron at 20°C is 344 m/s, 1485 m/s, and 5100 m/s, respectively. An audible acoustic wave with a frequency of 3 kHz has a wavelength in air of about 10 cm. However, acoustic waves with a much higher frequency, known as *ultrasound*, can have wavelengths down in the micrometer range. Using suitable acoustic lenses, *ultrasonic microscopy* is possible.

If sound or ultrasound is used for imaging, it is important to point out that propagation of sound is much more complex in solids. First, solids are generally not isotropic, and the elasticity of a solid cannot be described by a scalar compressibility. Instead, a tensor is required to describe the elasticity properties. Second, shear forces in contrast to pressure forces give rise also to *transversal acoustic waves*, where the deformation is perpendicular to the direction of propagation as with electromagnetic waves. Thus, sound waves of different modes travel with different velocities in a solid.

Despite all these complexities, the velocity of sound depends only on the density and the elastic properties of the medium. Therefore, acoustic waves show no dispersion (in the limit of continous mechanics, i. e., for wavelengths much large than distances between atoms). Thus waves of different frequencies travel with the same speed. This is an important basic fact for *acoustic imaging* techniques.

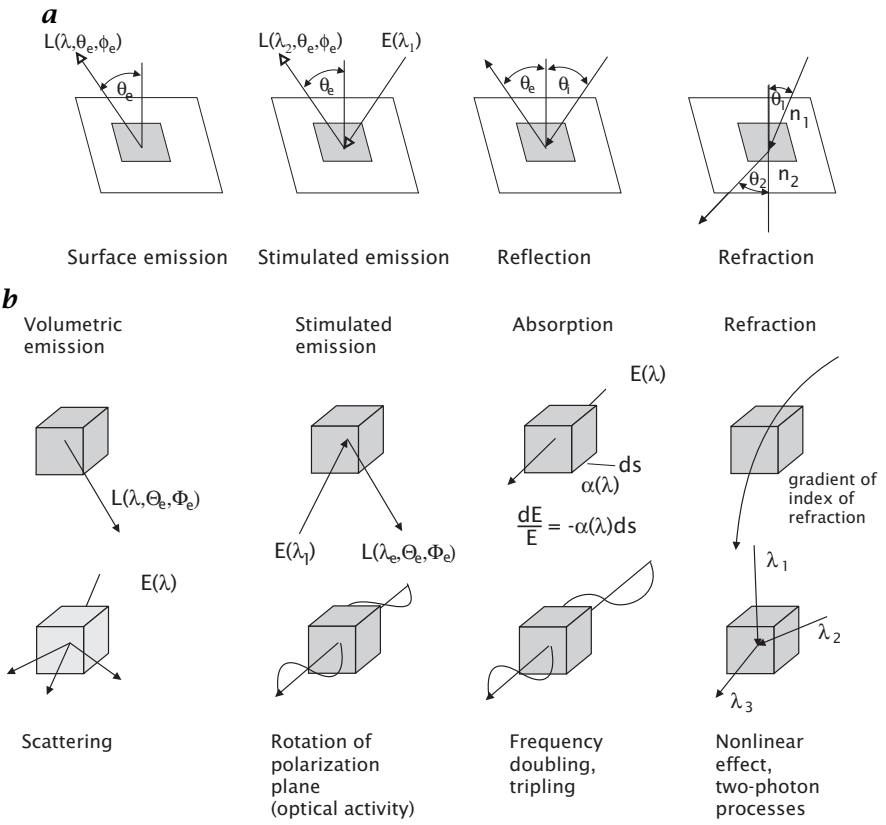

Figure 6.7: *Principle possibilities for interaction of radiation and matter:* ***a*** *at the surface of an object, i.e., at the discontinuity of optical properties,* ***b*** *volume related.*

6.4 *Interactions of Radiation with Matter*

The interaction of radiation with matter is the basis for any imaging technique. Basically, two classes of interactions of radiation with matter can be distinguished. The first class is related to the discontinuities of optical properties at the interface between two different materials (Fig. 6.7a). The second class is volume-related and depends on the optical properties of the material (Fig. 6.7b). In this section, we give a brief summary of the most important phenomena. The idea is to give the reader an overview of the many possible ways to measure material properties with imaging techniques.

6.4.1 *Thermal Emission*

Emission of electromagnetic radiation occurs at any temperature and is thus a ubiquitous form of interaction between matter and electromagnetic radiation.

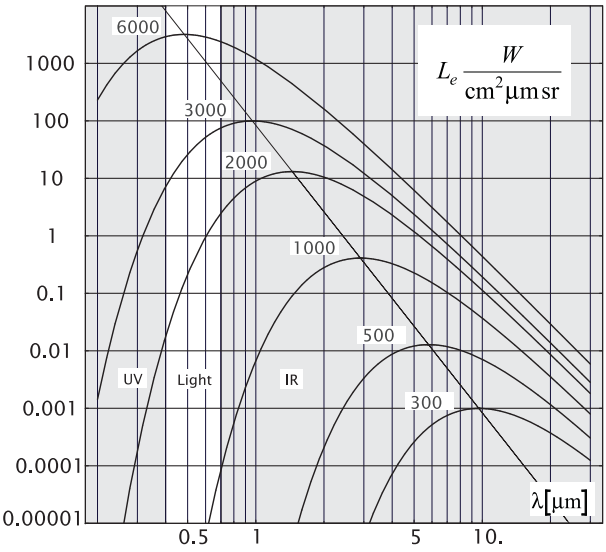

Figure 6.8: *Spectral radiance L_e of a blackbody at different absolute temperatures T in K as indicated. The thin line crosses the emission curves at the wavelength of maximum emission.*

The cause for the spontaneous emission of electromagnetic radiation is thermal molecular motion, which increases with temperature. During emission of radiation, thermal energy is converted to electromagnetic radiation and the matter is cooling down according to the universal law of energy conservation.

An upper level for thermal emission exists. According to the laws of thermodynamics, the fraction of radiation at a certain wavelength that is absorbed must also be re-emitted: thus, there is an upper limit for the emission, when the absorptivity is one. A perfect absorber — and thus a maximal emitter — is called a *blackbody*.

The correct theoretical description of the radiation of a blackbody by *Planck* in 1900 required the assumption of emission and absorption of radiation in discrete energy quanta $E = h\nu$. The spectral radiance of a blackbody with the absolute temperature T is (Fig. 6.8):

$$L_e(\nu, T) = \frac{2h\nu^3}{c^2} \frac{1}{\exp\left(\frac{h\nu}{k_B T}\right) - 1}, \quad L_e(\lambda, T) = \frac{2hc^2}{\lambda^5} \frac{1}{\exp\left(\frac{hc}{k_B T \lambda}\right) - 1}, \tag{6.24}$$

with

$$\begin{array}{ll} h = 6.6262 \times 10^{-34}\,\mathrm{J\,s} & \text{Planck constant,} \\ k_B = 1.3806 \times 10^{-23}\,\mathrm{J\,K^{-1}} & \text{Boltzmann constant, and} \\ c = 2.9979 \times 10^{8}\,\mathrm{m\,s^{-1}} & \text{speed of light in vacuum.} \end{array} \tag{6.25}$$

Blackbody radiation has the important feature that the emitted radiation does not depend on the viewing angle. Such a radiator is called a *Lambertian radiator*. Therefore the spectral emittance (constant radiance integrated over a

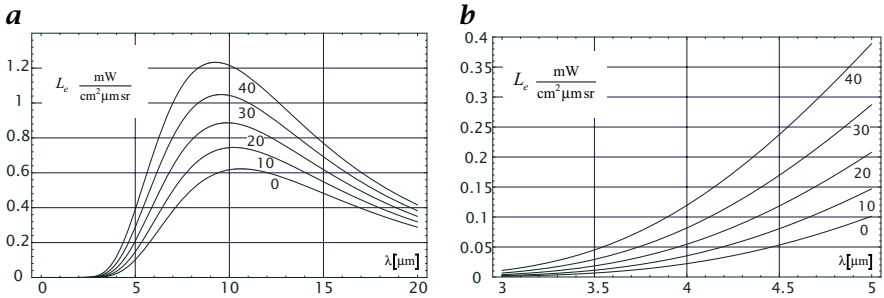

Figure 6.9: *Radiance of a blackbody at environmental temperatures as indicated in the wavelength ranges of* ***a*** *0–20 µm and* ***b*** *3–5 µm.*

hemisphere) is π times higher than the radiance:

$$M_e(\lambda, T) = \frac{2\pi hc^2}{\lambda^5} \frac{1}{\exp\left(\frac{hc}{k_B T \lambda}\right) - 1}. \tag{6.26}$$

The total emittance of a blackbody integrated over all wavelengths is proportional to T^4 according to the law of Stefan and Boltzmann:

$$M_e = \int_0^\infty M_e(\lambda)\,\mathrm{d}\lambda = \frac{2}{15}\frac{k_B^4 \pi^5}{c^2 h^3} T^4 = \sigma T^4, \tag{6.27}$$

where $\sigma \approx 5.67 \cdot 10^{-8}\mathrm{W\,m^{-2}K^{-4}}$ is the *Stefan–Boltzmann constant*. The wavelength of maximum emittance of a blackbody is given by *Wien's law*:

$$\lambda_m \approx \frac{2.898 \cdot 10^{-3}\mathrm{K\,m}}{T}. \tag{6.28}$$

The maximum excitance at room temperature (300 K) is in the infrared at about 10 µm and at 3000 K (incandescent lamp) in the near infrared at 1 µm.

Real objects emit less radiation than a blackbody. The ratio of the emission of a real body to the emission of the blackbody is called (specific) *emissivity* ϵ and depends on the wavelength.

Radiation in the *infrared* and *microwave* range can be used to image the *temperature distribution* of objects. This application of imaging is known as *thermography*. Thermal imaging is complicated by the fact that real objects are not perfect black bodies. Thus they partly reflect radiation from the surrounding. If an object has *emissivity* ϵ, a fraction $1 - \epsilon$ of the received radiation originates from the environment, biasing the temperature measurement. Under the simplifying assumption that the environment has a constant temperature T_e, we can estimate the influence of the reflected radiation on the temperature measurement. The total radiance emitted by the object, E, is

$$E = \epsilon\sigma T^4 + (1 - \epsilon)\sigma T_e^4. \tag{6.29}$$

This radiance is interpreted to originate from a blackbody with the apparent temperature T':

$$\sigma T'^4 = \epsilon\sigma T^4 + (1 - \epsilon)\sigma T_e^4. \tag{6.30}$$

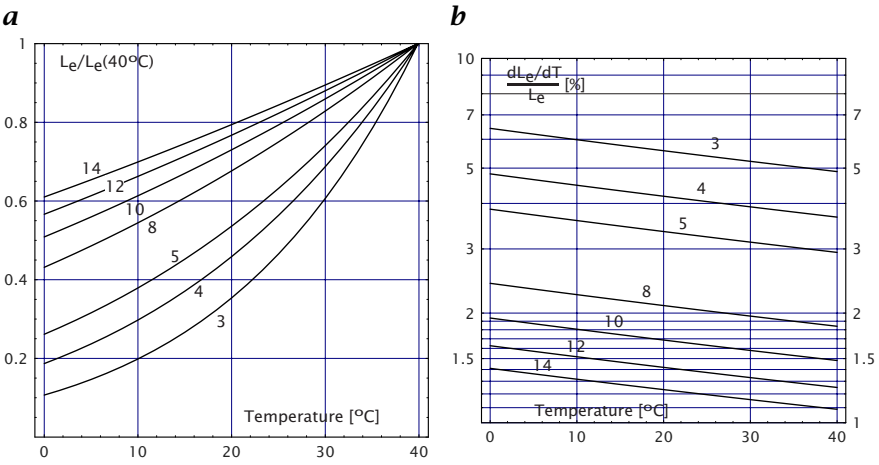

Figure 6.10: *Relative photon-based radiance in the temperature interval 0–40°C and at wavelengths in µm as indicated:* ***a*** *related to the radiance at 40°C;* ***b*** *relative change in percent per degree.*

Rearranging for T' yields

$$T' = T\left(\epsilon + (1-\epsilon)\frac{T_e^4}{T^4}\right)^{1/4}. \tag{6.31}$$

In the limit of small temperature differences ($\Delta T = T_e - T \ll T$) Eq. (6.31) reduces to

$$T' \approx \epsilon T + (1-\epsilon)T_e \quad \text{or} \quad T' - T \approx (1-\epsilon)\Delta T. \tag{6.32}$$

From this simplified equation, we infer that a 1% deviation of ϵ from unity results in 0.01 K temperature error per 1 K difference between the object temperature and the environmental temperature. Even for an almost perfect *blackbody* such as a water surface with a mean emissivity of about 0.97, this leads to considerable errors in the absolute temperature measurements. The apparent temperature of a bright sky can easily be 80 K colder than the temperature of a water surface at 300 K, leading to a $-0.03 \cdot 80\,\mathrm{K} = -2.4\,\mathrm{K}$ bias in the measurement of the absolute temperature of the water surface.

This bias can, according to Eqs. (6.31) and (6.32), be corrected if the mean temperature of the environment is known. Also relative temperature measurements are biased, although to a less significant degree. Assuming a constant environmental temperature in the limit $(T_e - T) \ll T$, we can infer from Eq. (6.32) that

$$\partial T' \approx \epsilon \partial T \quad \text{for} \quad (T_e - T) \ll T, \tag{6.33}$$

which means that the measured temperature differences are smaller by the factor ϵ than in reality.

Other corrections must be applied if radiation is significantly absorbed on the way from the object to the receiver. If the distance between the object and the camera is large, as for space-based or aerial infrared imaging of the Earth's

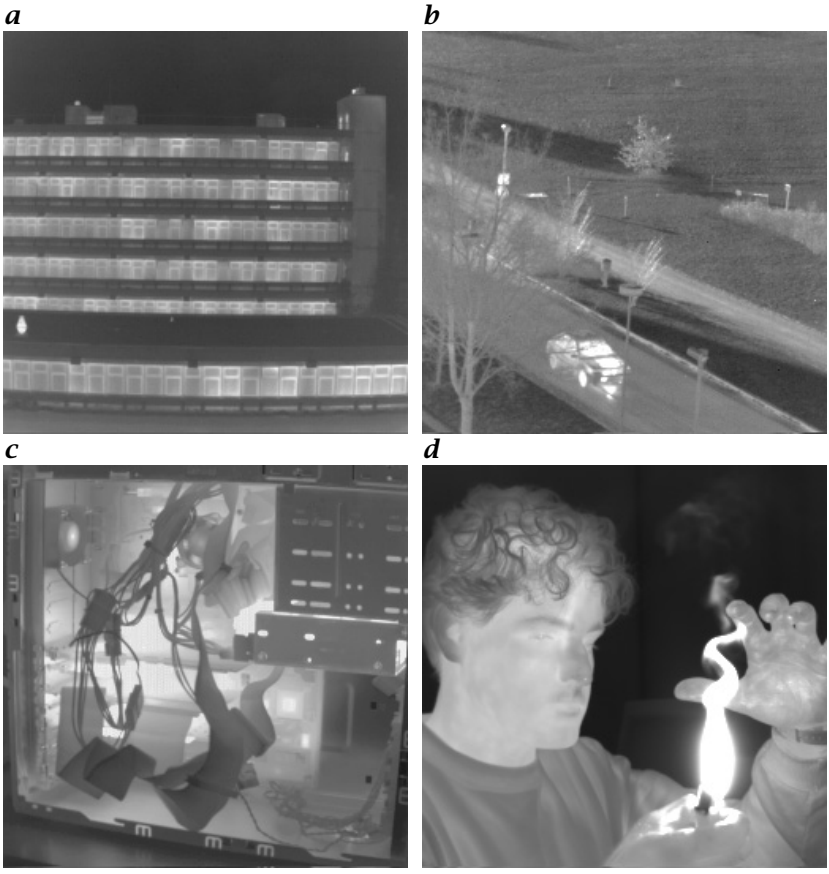

Figure 6.11: *Some examples of thermography:* ***a*** *Heidelberg University building taken on a cold winter day,* ***b*** *street scene,* ***c*** *look inside a PC, and* ***d*** *person with lighter.*

surface, it is important to select a wavelength range with a minimum absorption. The two most important atmospheric windows are at 3–5 μm (with a sharp absorption peak around 4.15 μm due to CO_2) and at 8–12 μm.

Figure 6.9 shows the radiance of a blackbody at environmental temperatures between 0 and 40 °C in the 0–20 μm and 3–5 μm wavelength ranges. Although the radiance has its maximum around 10 μm and is about 20 times higher than at 4 μm, the relative change of the radiance with temperature is much larger at 4 μm than at 10 μm.

This effect can be seen in more detail by examining radiance relative to the radiance at at fixed temperature (Fig. 6.10a) and the relative radiance change in $(\partial L/\partial T)/L$ in percent (Fig. 6.10b). While the radiance at 20°C changes only about 1.7 %/K at 10 μm wavelength, it changes about 4 %/K at 4 μm wavelength. This higher relative sensitivity makes it advantageous to use the 3–5 μm wavelength

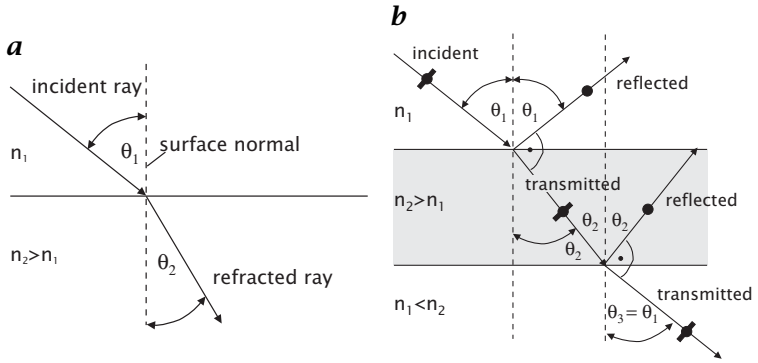

Figure 6.12: ***a*** *A ray changes direction at the interface between two optical media with a different index of refraction.* ***b*** *Parallel polarized light is entirely transmitted and not reflected when the angle between the reflected and transmitted beam would be 90°. This condition occurs at the transitions from both the optically thinner medium and the thicker one.*

range for measurements of small temperature differences although the absolute radiance is much lower.

Some images illustrating the application of *thermography* are shown in Fig. 6.11.

6.4.2 *Refraction, Reflection, and Transmission*

At the interface between two optical media, according to *Snell's law* the transmitted ray is refracted, i. e., changes direction (Fig. 6.12):

$$\frac{\sin\theta_1}{\sin\theta_2} = \frac{n_2}{n_1}, \tag{6.34}$$

where θ_1 and θ_2 are the angles of incidence and refraction, respectively. Refraction is the basis for transparent optical elements (lenses) that can form an image of an object. This means that all rays emitted from a point of the object and passing through the optical element converge at another point at the image plane.

A *specular surface* behaves like a mirror. Light irradiated in the direction (θ_i, ϕ_i) is reflected back in the direction $(\theta_i, \phi_i + \pi)$. This means that the angle of reflectance is equal to the angle of incidence and that the incident and reflected ray and the normal of the surface lie in one plane. The ratio of the reflected radiant flux to the incident flux at the surface is called the *reflectivity* ρ.

Specular reflection only occurs when all parallel incident rays are reflected as parallel rays. A surface need not be perfectly smooth for specular reflectance because of the wave-like nature of electromagnetic radiation. It is sufficient that the residual surface irregularities are significantly smaller than the wavelength.

The reflectivity ρ depends on the angle of incidence, the refractive indices, n_1 and n_2, of the two media meeting at the interface, and the polarization state of the radiation. Light is called parallel or perpendicular polarized if the electric

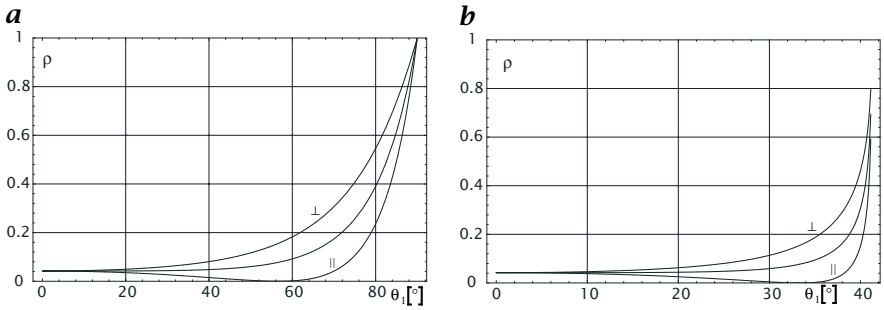

Figure 6.13: *Interface reflectivities for parallel (∥) and perpendicular (⊥) polarized light and unpolarized light incident from* ***a*** *air ($n_1 = 1.00$) to BK7 glass ($n_2 = 1.517$),* ***b*** *BK7 glass to air.*

field vector is parallel or perpendicular to the plane of incidence, i. e., the plane containing the directions of incidence, reflection, and the surface normal.
Fresnel's equations give the reflectivity for parallel polarized light:

$$\rho_{\parallel} = \frac{\tan^2(\theta_1 - \theta_2)}{\tan^2(\theta_1 + \theta_2)}, \tag{6.35}$$

for perpendicular polarized light

$$\rho_{\perp} = \frac{\sin^2(\theta_1 - \theta_2)}{\sin^2(\theta_1 + \theta_2)}, \tag{6.36}$$

and for unpolarized light (see Fig. 6.13)

$$\rho = \frac{\rho_{\parallel} + \rho_{\perp}}{2}, \tag{6.37}$$

respectively, where θ_1 and θ_2 are the angles of the incident and refracted rays related by Snell's law.
At normal incidence ($\theta_1 = 0$), the reflectivity does not depend on the polarization state:

$$\rho = \frac{(n_1 - n_2)^2}{(n_1 + n_2)^2} = \frac{(n-1)^2}{(n+1)^2} \quad \text{with} \quad n = n_1/n_2. \tag{6.38}$$

As illustrated in Fig. 6.13, parallel polarized light is not reflected at all at a certain angle, the polarizing or *Brewster angle* θ_b. This condition occurs when the refracted and reflected rays would be perpendicular to each other (Fig. 6.12b):

$$\theta_b = \arcsin \frac{1}{\sqrt{1 + n_1^2/n_2^2}}. \tag{6.39}$$

When a ray enters into a medium with lower refractive index, there is a critical angle, θ_c

$$\theta_c = \arcsin \frac{n_1}{n_2} \quad \text{with} \quad n_1 < n_2, \tag{6.40}$$

beyond which all light is reflected and none enters the optically thinner medium. This phenomenon is called *total reflection*.

6.4.3 *Rough Surfaces*

Most natural and also artificial objects do not reflect light directly but show a diffuse reflectance, as microscopic surface roughness causes reflection in various directions depending on the slope distribution of the reflecting facets. There is a great variety in how these rays are distributed over the emerging solid angle. Some materials produce strong forward scattering effects while others scatter almost equally in all directions. Other materials show a kind of mixed reflectivity, which is partly specular due to reflection at the smooth surface and partly diffuse caused by body reflection. In this case, light penetrates partly into the object where it is scattered at optical inhomogeneities. Part of this scattered light leaves the object again, causing a diffuse reflection. To image objects that do not emit radiation by themselves but passively reflect incident light, it is essential to know how the light is reflected.

Generally, the relation between the incident and emitted radiance can be expressed as the ratio of the radiance emitted at the polar angle θ_e and the azimuth angle ϕ_e and the irradiance received at the incidence angle θ_i. This ratio is called the *bidirectional reflectance distribution function* (*BRDF*) or reflectivity distribution, since it generally depends on the angles of both the incident and excitant radiance:

$$f(\theta_i, \phi_i, \theta_e, \phi_e) = \frac{L_e(\theta_e, \phi_e)}{E_i(\theta_i, \phi_i)}. \tag{6.41}$$

For a perfect mirror (specular reflection), f is zero everywhere, except for $\theta_i = \theta_e$ and $\phi_e = \pi + \phi_i$, hence

$$f(\theta_i, \theta_e) = \delta(\theta_i - \theta_e) \cdot \delta(\phi_e - \pi - \phi_i). \tag{6.42}$$

The other extreme is a perfect diffuser, reflecting incident radiation equally into all directions independently of the angle of incidence. Such a surface is known as *Lambertian radiator* or Lambertian reflector. The radiance of such a surface is independent of the viewing direction:

$$L_e = \frac{1}{\pi} E_i \quad \text{or} \quad f(\theta_i, \phi_i, \theta_e, \phi_e) = \frac{1}{\pi}. \tag{6.43}$$

6.4.4 *Absorptance and Transmittance*

Radiation traveling in matter is more or less absorbed and converted into different energy forms, especially heat. The absorptance is proportional to the radiant intensity in a thin layer $\mathrm{d}x$. Therefore

$$\frac{\mathrm{d}I(\lambda)}{\mathrm{d}x} = -\alpha(\lambda, x) I. \tag{6.44}$$

The *absorption coefficient* α is a property of the medium and depends on the wavelength of the radiation. It is a reciprocal length with the units m^{-1}. By integration of Eq. (6.44), we can compute the attenuation of radiation over the distance from 0 to x:

$$I(x) = I(0) \cdot \exp\left(-\int_0^x \alpha(\lambda, x')\mathrm{d}x'\right), \tag{6.45}$$

or, if the medium is homogeneous (i. e., α does not depend on the position x'),

$$I(x) = I(0)\exp(-\alpha(\lambda)x). \tag{6.46}$$

The exponential attenuation of radiation in a homogeneous medium, as expressed by Eq. (6.46), is often referred to as *Lambert–Beer's* or *Bouger's law*. After a distance of $1/\alpha$, the radiation is attenuated to $1/e$ of its initial value.

The path integral over the absorption coefficient

$$\tau(x_1, x_2) = \int_{x_1}^{x_2} \alpha(x')\mathrm{d}x' \tag{6.47}$$

results in a dimensionless quantity that is known as the *optical thickness* or *optical depth*. The optical depth is a logarithmic expression of radiation attenuation and means that along the path from the point x_1 to point x_2 the radiation has been attenuated to $e^{-\tau}$.

If radiation travels in a composite medium, often only one chemical species — at least at certain wavelengths — is responsible for the attenuation of the radiation. Therefore, it makes sense to relate the absorption coefficient to the concentration of that species:

$$\alpha = \varepsilon \cdot c, \quad [\varepsilon] = \left[\frac{\mathrm{l}}{\mathrm{mol\,m^{-1}}}\right], \tag{6.48}$$

where c is the concentration in mol/l. Then, ε is known as the *molar absorption coefficient*. The simple linear relation Eq. (6.48) holds for a very wide range of radiant intensities but breaks down at very high intensities, e. g., the absorption of highly intense laser beams. At that point, the domain of nonlinear optical phenomena is entered.

As the absorption coefficient is a distinct optical feature of chemical species, it can be used in imaging applications to identify chemical species and to measure their concentrations.

Finally, the term *transmittance* means the fraction of radiation that remains after the radiation has traveled a certain path in the medium. Often, transmittance and *transmissivity* are confused. In contrast to transmittance, the term transmissivity is related to a single surface. It means the fraction of radiation that is not reflected but enters the medium.

6.4.5 *Scattering*

The attenuation of radiation by scattering can be described with the same concepts as for loss of radiation by absorption. The scattering coefficient is defined by

$$\beta(\lambda) = -\frac{1}{I}\frac{\mathrm{d}I(\lambda)}{\mathrm{d}x}. \tag{6.49}$$

It is a reciprocal length with the units $\mathrm{m^{-1}}$. If in a medium the radiation is attenuated both by absorption and scattering, the two effects can be combined in the *extinction coefficient* $\kappa(\lambda)$:

$$\kappa(\lambda) = \alpha(\lambda) + \beta(\lambda). \tag{6.50}$$

Although scattering appears to be similar to absorption, it is a much more difficult phenomenon. The above formula can only be used if the radiation from the individual scattering events adds up incoherently at some point far from the particles. The complexity of scattering is related to the fact that the scattered radiation (without additional absorption) is never lost. Scattered light can be scattered more than once. Therefore, a fraction of it can reenter the original beam. The probability that radiance will be scattered in a certain path length more than once is directly related to the total attenuation by scattering along the path of the beam or the optical depth τ. If τ is smaller than 0.1, less than 10% of the radiance is scattered.

The total amount of scattered light and the analysis of the angular distribution is related to the optical properties of the scattering medium. Consequently, scattering is caused by the optical inhomogeneity of the medium. In the further discussion we assume that small spherical particles with radius r and index of refraction n are imbedded in a homogeneous optical medium.

Scattering by a particle is described by the *cross section*. It is defined in terms of the ratio of the flux removed by the particle to the flux incident on the particle:

$$\sigma_s = \phi_s / \phi \pi r^2. \tag{6.51}$$

The cross section has the units of area. It can be regarded as the effective area of the particle for scattering that completely scatters the incident radiative flux. Therefore, the *efficiency factor* for scattering Q_s is defined as the cross section related to the geometric cross section of the scattering particle:

$$Q_s = \sigma_s / (\pi r^2). \tag{6.52}$$

The angular distribution of the scattered radiation is given by the *differential cross section* $\mathrm{d}\sigma_s/\mathrm{d}\Omega$, i. e., the flux density scattered per unit solid angle. The total cross-section is given as the integral over the sphere of the differential cross-section:

$$\sigma_s = \int \frac{\mathrm{d}\sigma_s}{\mathrm{d}\Omega} \mathrm{d}\Omega. \tag{6.53}$$

The relation between the scattering coefficient β Eq. (6.49) and the scattering cross-section can be derived as follows. Let ρ be the number of particles per unit volume. Thus, the total effective scattering cross-section covers the area $\rho \cdot \sigma$. This area compared to the unit area gives the fraction of area that removes the incident flux and is thus equal to the scattering coefficient β:

$$\beta = \rho \sigma. \tag{6.54}$$

The scattering by small particles is most significantly influenced by the ratio of the particle size to the wavelength of the radiation expressed in the dimensionless particle size $q = 2\pi r/\lambda = 2\pi r k$. If $q \ll 1$ (Rayleigh scattering), the scattering is very weak and proportional to λ^{-4}:

$$\sigma_s / \pi r^2 = \frac{8}{3} q^4 \left| \frac{n^2 - 1}{n^2 + 2} \right|. \tag{6.55}$$

For $q \gg 1$, the scattering can be described by geometrical optics. If the particle completely reflects the incident radiation, the scattering cross-section is equal

to the geometric cross-section ($\sigma_s/\pi r^2 = 1$) and the differential cross-section is constant (isotropic scattering, $\mathrm{d}\sigma/\mathrm{d}\Omega = r^2/2$).

Scattering for particles with sizes of about the wavelength of the radiation (*Mie scattering*) is very complex due to diffraction and interference effects of the light scattered from different portions of the surface of the particle. The differential cross-section shows strong variations with the scattering angle and is directed mostly in the forward direction, while Rayleigh scattering is fairly isotropic.

6.4.6 *Optical Activity*

An optical material rotates the plane of polarization of electromagnetic radiation. The rotation is proportional to the concentration of the *optically active* material, c, and the path length d:

$$\varphi = \gamma(\lambda) c d. \tag{6.56}$$

The constant γ is known as the *specific rotation* and has the units [m^2 mol] or [cm^2 g^{-1}]; it depends strongly on the wavelength of the radiation. Generally, the specific rotation is significantly larger at shorter wavelengths.

Two well-known optically active materials are quartz crystals and sugar solution. Optical activity — including the measurement of the wavelength dependency — can be used to identify chemical species and to measure their concentration. With respect to visualization, optical activity is significant since it can be induced by various external forces, among others electrical fields (*Kerr effect*) and magnetic fields (*Faraday effect*).

6.4.7 *Luminescence*

Luminescence is the emission of radiation from materials that arises from a radiative transition from an excited state to a lower state. *Fluorescence* is luminescence characterized by short lifetimes of the excited state (on the order of nanoseconds), while the term *phosphorescence* is used for longer lifetimes (milliseconds to minutes).

Luminescence is an enormously versatile process because it can be triggered by various processes. In *chemiluminescence*, the energy required to generate the excited state is derived from the energy released by a chemical reaction. Chemiluminescence normally has only low efficiencies (i. e., number of photons emitted per reacting molecule) on the order of 1 % or less. Flames are the classic example of a low-efficiency chemiluminescent process. *Bioluminescence* is a chemiluminescence in living organisms. Fireflies and the glow of marine microorganisms are well-known examples. The firefly reaction involves the enzymatic oxidation of luciferin. In contrast to most chemiluminescent processes, this reaction converts almost 100 % of the chemical energy into radiant energy. Low-level bioluminescent processes are common to many essential biological processes. Imaging of these processes is becoming an increasingly important tool to study biochemical processes.

Marking biomolecules with fluorescent dyes is becoming another increasingly sophisticated tool in biochemistry. It has even become possible to mark individual chromosomes or gene sequences in chromosomes with fluorescent dyes.

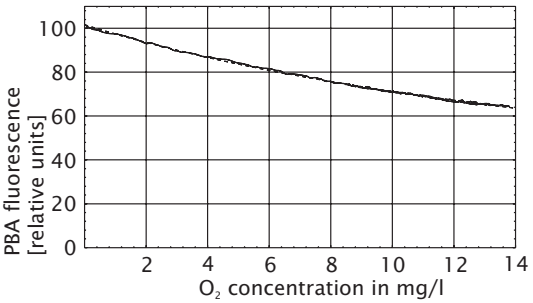

Figure 6.14: *Quenching of the fluorescence of pyrene butyric acid by dissolved oxygen: measurements and fit with the Stern–Vollmer equation (dashed line) [140].*

Luminescence always has to compete with other processes that deactivate the excited state without radiation emission. A prominent radiationless deactivation process is the energy transfer during the collision of molecules.

Some types of molecules, especially electronegative molecules such as *oxygen*, are very efficient in deactivating excited states during collisions. This process is referred to by the term *quenching*. The presence of a quenching molecule causes the fluorescence to decrease. Therefore, the measurement of the fluorescent irradiance can be used to measure the concentration of the quenching molecule. The dependence of the fluorescent intensity on the concentration of the quencher is given by the *Stern–Vollmer equation*:

$$\frac{L}{L_0} = \frac{1}{1 + kc_q}. \tag{6.57}$$

L is the fluorescent radiance, L_0 the fluorescent radiance when no quencher is present, C_q the quencher concentration, and k the quenching constant depending suitably on the lifetime of the fluorescent state. Efficient quenching requires that the excited state have a sufficiently long lifetime.

A fluorescent dye suited for quenching by dissolved oxygen is *pyrene butyric acid* (*PBA*) [206]. The relative fluorescent radiance of PBA as a function of dissolved oxygen is shown in Fig. 6.14 [141]. Fluorescence is stimulated by a pulsed nitrogen laser at 337 nm. The change in fluorescence is rather weak but sufficiently large to enable reliable measurements of the concentration of dissolved oxygen.

6.4.8 *Doppler Effect*

A velocity difference between a radiating source and a receiver causes the receiver to measure a frequency different from that emitted by the source. This phenomenon is known as the *Doppler effect*. The frequency shift is directly proportional to the velocity difference according to

$$\nu_r = \frac{c - \boldsymbol{u}_r^T \bar{\boldsymbol{k}}}{c - \boldsymbol{u}_s^T \bar{\boldsymbol{k}}} \nu_s \quad \text{or} \quad \Delta\nu = \nu_r - \nu_s = \frac{(\boldsymbol{u}_s - \boldsymbol{u}_r)^T \boldsymbol{k}}{1 - \boldsymbol{u}_s^T \bar{\boldsymbol{k}}/c}, \tag{6.58}$$

where $\bar{\boldsymbol{k}} = \boldsymbol{k}/|\boldsymbol{k}|$, ν_s is the frequency of the source, ν_r the frequency measured at the receiver, $\boldsymbol{k}$ the wave number of the radiation, c the propagation speed of the radiation, and $\boldsymbol{u}_s$ and $\boldsymbol{u}_r$ the velocities of the source and receiver relative to the medium in which the wave is propagating. Only the velocity component in the direction to the receiver causes a frequency shift.

If the source is moving towards the receiver ($\boldsymbol{u}_s{}^T\boldsymbol{k} > 0$), the frequency increases as the wave fronts follow each other faster. A critical limit is reached when the source moves with the propagation speed of the radiation. Then, the radiation is left behind the source. For small velocities relative to the wave propagation speed, the frequency shift is directly proportional to the relative velocity between source and receiver.

$$\Delta\nu = (\boldsymbol{u}_s - \boldsymbol{u}_r)\boldsymbol{k}. \tag{6.59}$$

The relative frequency shift $\Delta\omega/\omega$ is given directly by the ratio of the velocity difference in the direction of the receiver and the wave propagation speed:

$$\frac{\Delta\nu}{\nu} = \frac{(\boldsymbol{u}_s - \boldsymbol{u}_r)^T}{c}\bar{\boldsymbol{k}}. \tag{6.60}$$

For electromagnetic waves, the velocity relative to a "medium" is not relevant. The theory of relativity gives the frequency

$$\nu_r = \frac{\nu_s}{\gamma(1 - \boldsymbol{u}^T\bar{\boldsymbol{k}}/c)} \quad \text{with} \quad \gamma = \frac{1}{\sqrt{1 - (|\boldsymbol{u}|/c)^2}}. \tag{6.61}$$

For small velocities ($|\boldsymbol{u}| << c$), this equation also reduces to Eq. (6.59) with $\boldsymbol{u} = \boldsymbol{u}_s - \boldsymbol{u}_r$. In this case, acoustic and electromagnetic waves can be treated equally with respect to the frequency shift due to a relative velocity between the source and receiver.

6.5 *Exercises*

6.1: *Radiometric quantities

Which radiometric quantities describe the following processes:

1. the total radiometric energy emitted by a light source,
2. the radiometric power emitted by a light source per area and solid angle,
3. the radiometric energy received per area and time by an imaging sensor, and
4. the radiometric energy received per area and during an exposure time by an imaging sensor?

6.2: *Irradiance

A light source is mounted on a plane area and emits 1 W of radiometric power isotropically into the hemisphere. Which fraction of this power is received by a $10 \times 10\,\mu\text{m}^2$ imaging sensor element at a distance of 1 m? How large is the irradiance of the sensor element?

6.3: *Color mixing

Can pure (monochromatic) colors be produced by additive mixing of the three colors red, green, and blue?

6.4: *Metameric colors

Imagine a color sensor with three channels, red, green, and blue, that has either a spectral sensitivity corresponding to line sampling (Fig. 6.3a) or to band sampling (Fig. 6.3b) in Section 6.2.3. For each of the two sensor types, indicate at least three spectral distributions, which should be as different as possible from each other, that result in the same color perception.

6.5: *Color circle

Why do we perceive the color changes from red over yellow, green, and blue back to red again on a color circle as a continuous transition without discontinuities? Physically there is a discontinuity in the wavelength if we go from blue to red.

6.6: *Object features and radiation

Which parameters of the radiation emitted by an object and received by a camera can tell us about features of the observed object?

6.7: **Photons

How many photons are received by a $10 \times 10\,\mu\text{m}^2$ image sensor element that is irradiated with $E = 0.1\,\text{mW/cm}^2$ (about 1/1000 of the irradiation of direct sun light) for 1 ms? (Hint: the solution requires the Planck constant h, which has a value of $6.626 \cdot 10^{-34}$ Js.)

6.6 *Further Readings*

This chapter covered a variety of topics that are not central to image processing but are important to know for a correct image acquisition. You can refresh or extend your knowledge about electromagnetic waves by one of the classical textbooks on the subject, e. g., F. S. Crawford [41], Hecht [74], or Towne [201]. Stewart [195] and Drury [37] address the interaction of radiation with matter in the field of remote sensing. Richards [165] gives a survey of imaging techniques across the electromagnetic spectrum. The topic of infrared imaging has become an subject of its own and is treated in detail by Gaussorgues [56] and Holst [79]. Pratt [157] give a good description of color vision with respect to image processing. The practical aspects of photometry and radiometry are covered by the "Handbook of Applied Photometry" from DeCusaris [30]. The oldest application area of quantitative visualization is hydrodynamics. A fascinating insight into flow visualization with many images is given by the "Atlas of Visualization" edited by Nakayama and Tanida [143].